Clinical Significance of Prognostic Alternative Splicing Signature in Tumor Immune Environment and Immune Therapy of Hepatocellular Carcinoma

Qianhui Xu
Yuying Children's Hospital of Wenzhou Medical College: Wenzhou Medical University Second Affiliated Hospital
Hao Xu
Zhejiang University School of Medicine
Rongshan Deng
Zhejiang University School of Medicine
Nanjun Li
Zhejiang University School of Medicine
Ruiqi Mu
Zhejiang University School of Medicine
Zhixuan Qi
Zhejiang University School of Medicine
Yunuo Shen
Zhejiang University School of Medicine
Zijie Wang
Zhejiang University School of Medicine
Jingchao Wen
Zhejiang University School of Medicine
Jiaxin Zhao
Zhejiang University School of Medicine
Di Weng
Zhejiang University School of Medicine
Wen Huang (huangwen@wmu.edu.cn)
Yuying Children's Hospital of Wenzhou Medical College: Wenzhou Medical University Second Affiliated Hospital https://orcid.org/0000-0002-0010-3056

Primary research

Keywords: hepatocellular carcinoma, alternative splicing, tumor immune microenvironment, prognosis, immunotherapy

Posted Date: February 26th, 2021

DOI: https://doi.org/10.21203/rs.3.rs-252303/v1

Version of Record: A version of this preprint was published at Cancer Cell International on April 1st, 2021.
See the published version at https://doi.org/10.1186/s12935-021-01894-z.

Abstract

Background: Hepatocellular carcinoma (HCC) ranks the sixth prevalent tumors with high mortality globally. Alternative splicing (AS) drives protein diversity, the imbalance of which might act an important factor in tumorigenesis. We aimed to construct of AS-based prognostic signature and elucidate the role in tumor immune microenvironment (TIME) and immunotherapy in HCC.

Methods: To determine the prognosis-related AS events, univariate Cox regression analysis was performed, followed by the development of prognostic signatures. The prognosis predictive ability of risk signature was validated and a predictive nomogram was constructed. To uncover the context of TIME in HCC, ESTIMATE R package, ssGSEA algorithm and CIBERSORT method and TIMER database exploration were performed. And the correlation of AS events with immune checkpoint blockade (ICB)-related genes was analyzed.

Results: A total of 3294 AS events associated with survival of HCC patients were screened. Based on splicing subtypes, we then constructed eight AS prognostic signature with robust prognostic predictive accuracy. Furthermore, a quantitative nomogram exhibited robust validity in prognostic prediction of HCC. Besides, the consolidated signature was significantly correlated with TIME diversity and ICB-related genes. Finally, the splicing regulatory network uncovered the potential functions of splicing factors (SFs) in HCC.

Conclusion: Herein, the AS events may contribute novel and robust indicators for the prognostic prediction of HCC. The AS-SF networks could open up new approach for investigation of potential regulatory mechanisms. And we revealed the pivotal player of AS events in context of TIME and immunotherapy, contributing to clinical decision-making and personalized prognosis monitoring of HCC.

Introduction

Hepatocellular carcinoma (HCC) is a malignant and aggressive disease marked with frequently diagnosed and high cancer-attributable mortality in the world [1–3]. Despite great advance in HCC early diagnosis and anti-tumor therapy, clinical treatment result is still undesirable [4, 5]. Both tumor, node, metastasis (TNM) categories and Barcelona Clinic Liver Cancer (BCLC) staging classification, which were widely used prognostic tools, failed to precisely predict results of patients with same clinicopathological stage [6, 7]. Furthermore, the high heterogeneity of HCC remains great challenge against therapeutic benefits, which makes it difficult to accurately predict clinical result[1, 8].

A great part of HCC was derived from inflammatory liver diseases, which suggested that infiltrating immune cells in tumor immune microenvironment (TIME) might serve as pivotal regulatory roles in tumorigenesis and progression in HCC [9]. Recently, immunotherapy has received extensive attention since it yielded encouraging results in multiple malignancies [10]. However, only 20% of HCC patients were observed objective response to immunotherapy according to preclinical trials [11]. It is therefore

urgent to identify novel and reliable predictive indicator for enhanced prognostic precision and optimize immunotherapeutic benefit.

Alternative splicing (AS) defined as the mechanism by which edit pre-mRNA to produce mature mRNA, greatly contributed to the complexity of genome and the diversity of proteomic [12, 13]. It is well established that AS events included such main patterns as alternate acceptor site (AA), alternate donor site (AD), alternate promoter (AP), alternate terminator (AT), exon skip (ES), retained intron (RI) and mutually exclusive exons (ME) [14]. Unbalanced expression of AS occurs frequently in cancer and received extensive attention as pivotal role in tumor initiation, development, metastasis and response to treatment [15–17]. Besides, splicing factors were found to act as a vital player in the regulation of AS events [18]. It was worth mentioned that aberrant expression of crucial splicing factors can lead to the oncogenic splicing isoforms [19, 20].To date, multiple researches had been performed to unravel the biological relevance and clinical significance of AS events in HCC [21, 22]. There have been several articles focusing on AS-based prognostic model [23, 24], however, the correlation of AS prognostic signature with TIME and immunotherapy remains obscure.

Thus, it is imperative to perform a comprehensive analysis of AS events to uncover the characterization of TIME and underlying molecular mechanisms of tumorigenesis, further optimize clinical benefits.

In this study, we determined AS events associated with the survival of HCC patients through comprehensive bioinformatic analysis. Based on the AS events screened, we developed AS-based prognostic signatures and generated an AS-clinicopathologic nomogram to facilitate clinical application. Then, we explored the role of prognostic signature in the complexity of TIME and immunotherapeutic efficacy in HCC. Finally, we constructed an AS-SFs regulatory network to elucidate the potential mechanism involving in HCC progression.

Materials And Methods

Multiomic Data Acquisition

The transcriptome information and survival information of the HCC patients were downloaded from The Cancer Genome Atlas (TCGA) portal (http://cancergenome.nih.gov) for subsequent analysis. The alternative splicing data of TCGA LIHC-cohort were obtained from SpliceSeq (http://bioinformatics.

mdanderson.org/TCGASpliceSeq). We performed a screening filter of samples

with PSI value exceeds 0.75. All analyses were performed based on the publication guidelines of TCGA.

Process of AS profile identification

In TCGA splice-seq, we detected and calculated the percent spliced in (PSI) value to quantify AS events. By using UpsetR package, Upset plot was delineated to discovery the seven subtypes of AS events

(alternate acceptor site (AA), alternate donor site (AD), alternate promoter (AP), alternate terminator (AT), exon skip (ES), mutually exclusive exons (ME), and retained intron (RI)). The AS events were annotated by combining the splicing type, ID number in the SpliceSeq and the corresponding parent gene symbol. For example, in “MRPL43|12849|AT”, MRPL43 denotes the corresponding parent gene name, 12849 represents the ID of splicing variant and AT indicates the splicing type.

Identification of survival-related AS events

When the standard deviation of PSI value is less than 0.01, the AS data were excluded. Univariate Cox regression analysis was carried out to detect the association between AS events and overall survival (OS) of HCC patients (Table S1), which were presented with the UpSet plot and the volcano map. Besides, the top 20 most significant AS events from the seven subtypes were summarized in the bubble charts.

Construction and validation of prognostic signature

Firstly, Lasso regression analysis was employed to determine candidates in each splicing pattern and avoid model over-fitting. Secondly, the identified AS events were introduced into Multivariate Cox regression analysis to screen the prognostic predictor. Given the mode of AS events is independent from each subtype in post-transcriptional modification, the identified AS events in each splicing subtype above were integrated to generate another prognostic signature. Subsequently, the risk scores were calculated according to each prognostic predictor and the formula for computing the risk score is as follows: Risk score = βAS event1 × PSIAS event1 + βAS event2 × PSIAS event2 + ⋯ + βAS eventn × PSIAS eventn. The specific formulas of each signature were presented in Table S2. Based on the median value of risk score, patients were ranked into low-risk group and high-risk group. Kaplan–Meier survival curves were analyzed with “survival” R package. Then, the time-dependent receiver operating characteristic (ROC) curves were performed to examine the prognostic value of this signature. Besides, univariate and multivariate Cox regression were analyzed to confirm whether the signature can serve as an independent factor for prognostic prediction. Then, stratified survival analysis was conducted to further validate the prognostic performance independent from such clinical characteristics as age, gender, tumor stage, pathological grade, T category, N category and M category.

Construction of Prognostic Nomogram

To comprehensively assess prognosis predictive ability of risk signature, tumor stage, gender, age, WHO grade, T category, N category and M category for 1/2/3-year OS, time-dependent receiver operating characteristic (ROC) curves was perform to calculate the area under the curve (AUC) values [25]. To contribute a quantitative manner to predicting overall survival of patients with HCC, we established a nomogram that containing this AS-based risk model and other clinical variables to estimate 1-, 2-and 3-year overall survival probability. Subsequently, we analyzed the calibration curve which shown the

prognostic value of as-constructed nomogram. A calibration curve close to 45° is an indication of good prediction ability of the model constructed by this factor.

Correlation of risk score with Tumor Infiltrating Immune Cells Characterization

Immune infiltration information consists of every specimen immune cell fraction (i.e., B cells, CD4+T-cells, CD8+T-cells, dendritic cells, macrophages, and neutrophils, etc.,) were downloaded from tumor immune estimation resource (TIMER) (https://cistrome.shinyapps.io/timer/). The correlation between tumor immune cell infiltrating with the prognostic risk score was performed. A single sample gene-set enrichment analysis (ssGSEA) was employed to elucidate the enrichment of the two distinct risky subgroups in 29 immune function-associated gene sets via invoking the R package “GSEAbase”. Subsequently, the R package “ESTIMATE” was employed to assess tumor purity and the extent and level of infiltrating cells, namely stromal cell and immune cell, that could validate significant distinct tumor immune microenvironment characterization between two risky subgroups. The fraction of 22 immune cell types for each tumor specimen was developed through cell type identification by estimating relative subsets of RNA transcripts (CIBERSORT; https://cibersort.stanford.edu/).

Role of risk score in Immune Checkpoint Blockade Treatment

Refer to existing studies, expression level of immune checkpoint blockade-related key genes might be correlated with clinical outcome of immune checkpoint inhibitors blockade treatment[26]. Herein, we employed six key genes of immune checkpoint blockade therapy: programmed death ligand 1 (PD-L1, also known as CD274), programmed death ligand 2 (PD-L2, also known as PDCD1LG2), programmed death 1 (PD-1, also known as PDCD1), cytotoxic T-lymphocyte antigen 4 (CTLA-4), indoleamine 2,3-dioxygenase 1 (IDO1), and T-cell immunoglobulin domain and mucin domain-containing molecule-3 (TIM-3, also known as HAVCR2) in HCC[27-29]. To elucidate the potential player of as-constructed risk signature in ICB treatment of HCC, we correlated AS-based prognostic signature and expression level of six immune checkpoint blockade key genes. Finally, we systematically compared the expression level of 47 immune checkpoint blockade-related genes (i.e., PDCD1, etc.,) between low-/high-risk groups.

Construction of splicing regulatory network

A list of 404 splicing factors (SFs, Table S3) was referred to a previous research[30] and the RNA-seq profiles of SFs were downloaded from the TCGA database. The Spearman correlation analysis was performed to evaluate the association between the SFs and the survival-relevant AS events(Table S4). P <

0.001 and Correlation coefficient > 0.6 was the cutoff values. Finally, Cytoscape (version 3.8.0) was employed to build an underlying SF-AS regulatory network.

Experimental Validation

L02 cell (human hepatic cell line) and two human HCC cell lines (MHCC-97H cells and HCC-LM3) were purchased from the Cell Bank of the Type Culture Collection of the Chinese Academy of Sciences, Shanghai Institute of Biochemistry and Cell Biology. The cell lines were all cultured in Dulbecco's minimum essential media (DMEM) plus 10% fetal bovine serum (FBS; Invitrogen, Carlsbad, CA, USA). All cell lines were grown without antibiotics in a humidified atmosphere of 5% CO2 and 99% relative humidity at 37℃. Three different cell lines were subjected to quantitative real-time polymerase chain reaction (qRT-PCR).

RNA Isolation and qRT-PCR Analysis

Total RNA was extracted from cells using TRIzol (Invitrogen, Carlsbad, CA, USA) according to provided instructions. RNA concentration and purity were measured in triplicates utilizing the NanoDrop 2000 spectrophotometer (Thermo Scientific Inc., Waltham, MA, 93 USA). Then, total RNA was reverse transcribed to cDNA using the cDNA Reverse Transcription Kit (Vazyme, Nanjing, China). To determine the expression of ZDHHC16, cDNAs were subjected to qRT-PCR using SYBR Green Real-time PCR Master Mix (Takara) in Applied Biosystems 7500/7500 Fast Real-Time PCR System (Thermo Fisher Scientific). All samples were analyzed in triplicates. Glyceraldehyde-3-phosphate dehydrogenase (GAPDH) levels were used as the endogenous control and relative expression of ZDHHC16 was calculated using the 2-ΔΔCt method. The sequences of primers used for PCR were as follows: ZDHHC16, 5'-CCACCAGACTCCACCACCTACC -3' (forward) and 5'-GCCACAGAACTGCACAGGAACC -3' (reverse); and GAPDH, 5'-CAGGAGGCATTGCTGATGAT-3' (forward) and 5'-GAAGGCTGGGGCTCATTT-3' (reverse).

Statistical Analysis

The Wilcoxon test was employed to compare two groups, whereas the Kruskal-Wallis test was carried out to compare more than two groups. Overall survival (OS) refers to the interval from the date of diagnosis to the date of death. Survival curves were plotted via the Kaplan-Meier log rank test. Risk scores, clinical variables, immune cell infiltrating extent and immune checkpoints were correlated with Pearson correlation test. CIBERSORT algorithm results with p>=0.05 were rejected for further analysis. Univariate and multivariate analyses were performed via Cox regression models to validate the independent prognosis predictive performance of risk signature. The prognostic value of the AS-based signatures for 1-, 2- and 3-year OS was assessed with the ROC curves. $p < 0.05$ deemed statistical significance. R software (version 4.0.2) was utilized for all statistical analyses.

Results

Clinical characteristics and Integrated AS Events Profiles in HCC

377 HCC patients were obtained using the TCGA database, and seven patients with incomplete information were excluded from this study. In total, 370 patients were enrolled. The basic clinical information of patients is shown in Table 1. The AS events profiles were comprehensively analyzed and the gene intersections among the seven subtypes of AS events was presented in UpSet plot (Figure S1A). These results showed that ES was the predominant splicing pattern meanwhile AD marked as the least frequent.

Identification of the survival-relevant AS events

With the help of Univariate Cox regression analysis, we identified a total of 3294 AS events which were significantly related with survival ($P<0.05$). The detailed description was recorded in Table S1. The intersecting sets of genes and splicing subtypes were delineated in the UpSet plot (Figure S1B). Among these subtypes of AS events, ES was the predominant pattern. The volcano map was generated to display the AS events (Figure 1A). The first 20 significant survival-related AS events from the seven subtypes were summarized in Figures 1B-H.

Development of the Prognostic Signature

Stepwise Lasso algorithm and multivariate Cox regression analysis were employed to estimate the prognostic performance of these identified survival relevant AS events. The results of Lasso regression analysis including seven subtypes of AS events and amalgamated AS events with seven splicing types were displayed in Figures S2A-S2G, S3A-S3G and 2A-2B. Then, we performed multivariate Cox analysis to determine optimal survival-relevant AS events. Lastly, eight AS (AA, AD, AP, AT, ES, ME, RI, and ALL) prognostic signature were constructed. Table 2 presented the detailed formulas of each signature.

Confirmation of the Prognostic Signature

Based on the cut-off value of median risk score, HCC patients were stratified into low and high-risk subgroups for further research. Heatmaps displayed the distributions of AS events PSI values with corresponding subgroups and patients (Figures S4A, S4D, S5A, S5D, S6A, S6D, S7A and 2C). The allocations of risk score (Figures S4B, S4E, S5B, S5E, S6B, S6E, S7B and 2D) and dot pot of survival status (Figures S4C, S4F, S5C, S5F, S6C, S6F, S7C and 2E) suggested that high-risk HCC patients had shorter overall survival. Besides, Kaplan–Meier curve corroborated that patients with low-risk possessed significant better prognosis than patients in high-risk group (Figures S8A, S8C, S8E, S8G, S9A, S9C, S9E

and 2F; all P<0.05). To assess the prognostic value of risk signatures in HCC cohort, we performed ROC curve analysis. Area under curves of risk scores at 1-, 2- and 3-year survival times were all more than 0.7, suggesting great sensitivity and specificity of their survival predictive ability (Figures S8B, S8D, S8F, S8H, S9B, S9D, S9F and 2G). Besides, results of univariate Cox model (Figures S10A, S10B, S10C, S10D, S10I, S10J, S10K and 2H) and multivariate Cox regression analysis (Figures S10E, S10F, S10G, S10H, S10L, S10M, S10N and 2I), suggesting risk scores could act an independent indicator in HCC.

We performed a stratification analysis to validate whether ALL prognostic signature still had powerful prognostic predictive ability when HCC patients classified into various subgroups based on clinical characteristics. Relative to patients with low-risk, high-risk HCC patients presented poorer prognosis in both the early- and late-stage subgroups (Figures S11A, S11B). Similarly, ALL prognostic signature presented excellent prognostic prediction performance for patients in T1-2 or T3-4 status (Figures S11C and S11D), patients male or female gendered (Figures S11E, S11F), patients in 1-2 or 3-4 tumor grade (Figures S11G, S11H), patients aged <=65 years or >65 years (Figures S11I, S11J), patients in N0 status (Figures S11K), and patients in M0 status (Figures S11L). These results suggested that it can be an outstanding predictor independent from clinical parameters in patients with HCC.

Confirmation of Prognostic Value of ALL prognostic signature

We compared risk score among different subtypes according to clinical variables. The risk score increased significantly with advanced tumor grade (most P<0.05, Figures 3A), advanced clinicopathological stage (most P<0.05, Figures 3B) and advanced T category (most P<0.05, Figures 3C). To explore whether ALL prognostic signature was the best prognostic indicator among various clinical characteristics, age, gender, clinicopathological stage, tumor grade, T status, N status and M status were extracted as the candidate prognosis predictive factors. We integrated these clinical variables then conducted the AUC curve analysis for 1-, 2-, and 3-year OS and observed that risk signature obtained the most AUC (Figures 3D, 3E, and 3F). We generated a nomogram including risk score and clinicopathological stage to forecast prognosis of patients with HCC (Figure 3G). Age, gender and tumor grade were rejected out of the nomogram because of their AUCs were less than 0.6. Calibrate curves indicated powerful prognostic predictive ability of 1-, 2- and 3-year OS in our nomogram plot (Figure 3H-I).

Correlation of Risk Score with Tumor Immune Environment Characterization

To further examine whether risk score can act as immune indicators in both TCGA and ICGC HCC datasets, we performed the correlation analysis of prognostic risk score with TICs from TIMER, immune score (calculated using the ESTIMATE algorithm), ssGSEA signatures and TICs subtype and level (calculated via CIBERSORT method). Firstly, TIMER results showed that the as-constructed signature

exhibited the marked positive association with B cells infiltration(r = 0.116; p =0.026), CD8+T cells infiltration(r = 0.223; p =2.349e−05), Dendritic cells infiltration(r = 0.228; p = 1.564e−05), Macrophages infiltration(r = 0.271; p =2.357e−07) and Neutrophils infiltration(r = 0.221; p = 2.945e−05; Figures 4A-D). We found that low-risk patients obtained a higher stromal score compared with high-risk HCC patients (Figure 4F). However, there was no significant difference regarding to immune score, estimate score and tumor purity (Figures S12A, S12B and S12C). Subsequently, we distinguished distinction of the immune-related signatures between these two subgroups. Figure 4G and 4H showed that immune-related signature of each patient with corresponding immune scores in low-/high-risk groups. We observed that the infiltration of aDCs, Macrophages, Neutrophils, Tfh, Th1 cells, Th2 cells, Tregs, and some immune signatures like APC costimulation, T cells costimulation, check-point, HLA molecule expression level, inflammation-promoting, MCH class I expression and IFN response were significantly increased with decreased risk score (Figure 4I). The CIBERSORT algorithm results indicated that proportion of reseing Dendritic cells was negatively associated with risk score (Figure 4J). Above results indicated that ALL prognostic signature may provide a novel approach to elucidate the characteristics of immunity regulatory network in HCC.

Correlation of ALL Signature with ICB Key Molecules

With the emergence of immune checkpoint blockade (ICB) therapy, immune checkpoint inhibitors have considerably transformed clinical decision-making in cancer oncology [31-33]. Subsequently, we correlated six key immune checkpoint inhibitors genes (PDCD1, CD274, PDCD1LG2, CTLA-4, HAVCR2, and IDO1) [27-29]. And we analyzed the correlation between ICB key targets and ALL prognostic signature to reveal the potential player of risk signature in the ICB treatment of HCC (Figure 5A). We found that ALL prognostic signature was significantly positive correlated to CD274 (r= 0.26; P= 0.00015), CTLA4 (r= 0.33; P= 1.3e−06), HAVCR2 (r= 0.41; P= 1.4e−09), IDO1 (r= 0.15; P= 0.03), PDCD1 (r= 0.16; P= 0.021) and PDCD1LG2 (r = 0.23; P = 0.001; Figures 5B-H). Further correlation analysis presented that 33 of 47 (i.e., PDCD1, CTLA4, etc.,) immune check blockade-associated genes expression levels were significantly upregulated in patients with high-risk (Figure 5G), suggesting ALL prognostic signature might act a nonnegligible role in the prediction of responsiveness to ICB treatment in patients with HCC

ZDHHC16 Independently Affected Prognosis and Correlated with ICB key Genes

ZDHHC16 was only one gene whose expression level was upregulated among the prognostic AS-related genes. Therefore, the role of ZDHHC16 in HCC was explored in further experimental validation. We compared ZDHHC16 expression level between normal tissues and tumor samples based on TCGA data. Relative to tumor tissues, ZDHHC16 expression level was lower in adjacent normal specimens (Figure 6A). Taking advantage of qRT-PCR, we determined ZDHHC16 expression level in two distinct HCC cell lines and human hepatic cell line. Consistent of results of online database, ZDHHC16 was upregulated in

cancer cells relative to normal cell (Figure 6B). The expression level analysis among major pathological stages presented that ZDHHC16 expressed statistical significantly among different pathological stages (Figure 6C, F= 3.45 and P= 0.0168). And we found that the later tumor grade, the higher risk score (Figure 6D, almost P<0.05). To further assess the prognostic value of ZDHHC16 in HCC, Kaplan–Meier analysis were conducted between ZDHHC16 low- and high-expressed patients. As presented in Figures 7E and 7F, lower ZDHHC16 expression level significantly suggested longer overall survival time (P = 0.0056) and longer disease-free survival time (P = 0.02). We compared 47 immune check blockade-associated genes expression levels between low-ZDHHC16 and high-ZDHHC16 groups and observed that 16 of 47 (i.e., PDCD1, CTLA4, etc.,) immune check blockade-associated genes expression levels were significantly dysregulated in between different subgroups (Figure 6G). Then we performed the correlation between the ZDHHC16 and ICB key targets adjusted by tumor purity by TIMER to investigate the potential player of ZDHHC16 in ICB treatment of HCC. TIMER results presented ZDHHC16 was significantly positive correlated to CD274 (r= 0.132; P = 1.41e−02), CTLA4 (r= 0.254; P = 1.79e−06), HAVCR2 (r= 0.231; P = 1.50e−05) and PDCD1 (r = 0.291; P = 3.66e−08; Figures 6H-K), suggesting ZDHHC16 may exert a vital player in ICB treatment of HCC.

Development of the SF-AS regulatory Network

To elucidate the underlying mechanism of AS regulation, we generated a correlation network between the expression level of SFs and the PSI values of prognosis-related AS events. We identified 55 up-regulated AS events (yellow ellipses), 56 down-regulated AS events (blue ellipses) and 106 SFs (Figure 7). In our regulatory network, the top four most significant nodes were termed as the hub SFs or AS events (Table S), including one downregulated AS event (ACAA1-64022-ES), one upregulated AS events (SCP2-3045-ES) and two SFs (ISY1 and CLK2). As such, we speculated that these SFs served as pivotal regulators involving in the dysregulation of AS in HCC, further mediated tumor initiation and progression.

Discussion

As one of the most common type of malignant tumor, hepatocellular carcinoma (HCC) had high cancer-relevant mortality globally [1–3]. Since such intricate molecular mechanism as genomic complexities and epigenetic diversities, HCC was highly heterogeneous from both clinical standpoint and molecular level [34–36]. A sober reality is that a majority of HCC patients cannot obtain benefit from immunotherapy, due to tumor-promoting condition mediated by immunosuppressive cells (i.e., regulatory T cells, etc.,) [37]. Thus, there is an urgent call to develop powerful prognostic tools for immunotherapeutic outcome prediction, which could contribute novel insight into individual tailored treatment in HCC.

Increasing studies have provided strong evidence to support that AS, which refers to post-transcriptional modification procedure, function in physiological and pathological process [12]. Notably, abnormally regulated AS events participated well in tumor initiation and development, including HCC [16, 38]. Furthermore, dysregulated expressed genes can be employed as novel prognostic indicator and

promising therapeutic targets. However, little to know the correlation of AS events with context of TIME and immunotherapeutic results in HCC.

In current study, we obtained AS data from TCGA SpliceSeq and performed a comprehensive analysis of AS events in HCC samples. Taking advantage of univariate Cox regression analysis, we identified 3294 AS events significantly associated with the survival to explore the prognostic value of AS events. Next, we proposed prognostic signatures for HCC patients. All eight (AA, AD, AP, AT, ES, ME, RI, and ALL) prognostic predictive signatures constructed by AS patterns presented powerful capability for the prognostic prediction in HCC. Notably, these AS-based prognostic signatures were robustly demonstrated by K-M survival analysis, ROC curve and Cox regression analysis. Furthermore, we validated this signature retain excellent prognostic performance when HCC cases divided into groups based on clinicopathological factors. To transform ALL risk model into further clinical practice, a nomogram graph consolidated prognostic signature with clinicopathological stage was plotted, and we observed high consistence between predicted outcome and actual outcome. Besides, the most significant associated SF-AS regulatory network in the TCGA LIHC cohort were screened.

To reveal the role of AS events in the context of TIME in HCC, TIMER database, ESTIMATE algorithm, ssGSEA method and CIBERSORT analysis were conducted. Collectively, these results presented that high-risk score group was marked with high infiltration of immune cells and more activated immune condition, which might promote immune recognition and trigger anti-tumor effect. These outcomes implied that the risk score in our research might facilitate immunotherapy results prediction. Since no ICB treatment dataset in HCC cohort, we were unable to investigate the relationship between risk score and ICB immunotherapy response. Then we observed that risk score was positively and significantly correlated with six ICB key targets (i.e., CD274 and CTLA4) and 33 (i.e., PDCD1LG2, etc.,) immune check blockade-associated genes expression levels, which imply that risk score might contribute to strategizing the tailored immunotherapy.

ZDHHC16 was a DHHC encoding protein, which was tightly correlated with protein palmitoylation in previous researches[39]. Wei Shi et al. reported that ZDHHC16 acted as a vital regulator in the process of NSPCs proliferation[40]. Li Jian et al. uncovered pivotal players for ZDHHC16 in the regulation of DNA damage responses and Atm activation[41]. To date, little to know about the role of ZDHHC16 in tumors, especially in HCC. This study presents that ZDHHC16 is significantly upregulated in HCC cell lines and suggested poor prognosis in HCC. ZDHHC16 expression was significantly positive associated with clinicopathological stage, tumor grade and ICB immunotherapy key genes(i.e., CD274, CTLA4, HAVCR2 and PDCD1, etc.).Nevertheless, we need to perform further research to explore the underlying biological roles of ZDHHC16.

Compared this research with existed studies that explored the novel prognostic factor in HCC, some superiorities of our research should be noted. Firstly, all HCC cases from TCGA database were included for thoroughly analysis, and the total specimen size was considerably large. Besides, we contribute to investigate the potential roles of AS events in formation of TIME diversity and complexity and ICB

treatment prediction, which has not been elucidated before this study. Finally, to our knowledge, this work is the first focusing on the biological functions of ZDHHC16 in HCC.

Conclusion

Collectively, we systematically analyzed the prognosis predictive value, and impacts on TIME and ICB treatment of RNA splicing patterns in HCC. It is worthwhile mentioned that we provided a novel and robust nomogram to predict outcome quantitatively, which exhibited encouraging potential into clinical application. The AS-SFs regulatory network suggested a promising target of the anti-tumor therapy in HCC. The difference of AS patterns was a factor that was closely correlated with prognosis and clinicopathological parameters, suggesting it could serve as crucial role in the complexity and heterogeneity of tumor microenvironment. The comprehensive analysis of AS events robustly linked the AS atlas with TIME and immunotherapy in HCC. Nevertheless, our findings should be confirmed in further experimental and clinical exploration which focusing on HCC tumorigenesis and progression mechanisms and the impacts of these AS events.

Abbreviations

AA
alternate acceptor site
AD
alternate donor site
AP
alternate promoter
AT
alternate terminator
AUC
area under the curve
AS
alternative splicing
BCLC
Barcelona Clinic Liver Cancer
CTLA-4
cytotoxic T-lymphocyte antigen 4
CD274
Also known as PD-L1
DMEM
Dulbecco’s minimum essential media
ES
exon skip

FBS
fetal bovine serum
GAPDH
glyceraldehyde-3-phosphate dehydrogenase
GO
Gene ontology
HCC
hepatocellular carcinoma
HAVCR2
Also known as TIM3
IDO1
indoleamine 2,3-dioxygenase 1
ICB
immune checkpoint blockade
LASSO
least absolute shrinkage and selection operator
ME
mutually exclusive exons
OS
overall survival
PD-1
Programmed Cell Death 1
PD-L1
Programmed Cell Death-Ligand 1
PD-L2
Programmed Cell Death-Ligand 2
PDCD1
Also known as PD-1
PDCD1LG2
Also known as PD-L2
qRT-PCR
quantitative real-time polymerase chain reaction
RI
retained intron
RNA
Ribonucleic Acid
ROC
receiver operating characteristic
SFs
splicing factors

ssGSEA
single-sample gene set enrichment analysis
TCGA
The Cancer Genome Atlas
TICs
tumor-infiltrating immune cells
TIME
tumor immune microenvironment
TIMER
tumor immune estimation resource
TIM-3
T-cell immunoglobulin domain and mucin domain-containing molecule-3
TNM
tumor, node, metastasis

Declarations

Ethics approval and consent to participate

Not applicable

Consent for publication

Not applicable.

Availability of data and materials

The study was based on the data available at TCGA(https://www.cancer.gov/tcga).

Competing interests

The authors declare that they have no competing interests.

Funding

This research did not receive any specific grant from funding agencies in the public, commercial, or not-for-profit sectors.

Authors' contributions

HW designed the overall study and revised the paper, XQH performed public data interpretation, XH drafted manuscript. DRS supervised the experiments. LNJ, MRQ and QZX participated in data collection, SYN, WZJ and WD contributed to data analysis, WJC and ZJX participated in the molecular biology experiments. All authors

read and approved the final manuscript.

*Qianhui Xu, and Hao Xu contributed equally to this paper.

Acknowledgements

The authors would like to give our sincere appreciation to the reviewers for their helpful comments on this article and research groups for the TCGA, which provided data for this collection. This research did not receive any specific grant from funding agencies in the public, commercial, or not-for-profit sectors.

References

1. Forner A, Reig M, Bruix J. Hepatocellular carcinoma. Lancet. 2018;391:1301–14.
2. Bray F, Ferlay J, Soerjomataram I, Siegel R, Torre L, Jemal A. Global cancer statistics 2018: GLOBOCAN estimates of incidence and mortality worldwide for 36 cancers in 185 countries. Cancer J Clin. 2018;68:394–424.
3. Yang J, Hainaut P, Gores G, Amadou A, Plymoth A, Roberts L. A global view of hepatocellular carcinoma: trends, risk, prevention and management. Nat Rev Gastroenterol Hepatol. 2019;16:589–604.
4. Song P, Cai Y, Tang H, Li C, Huang J. The clinical management of hepatocellular carcinoma worldwide: A concise review and comparison of current guidelines from 2001 to 2017. Biosci Trends. 2017;11:389–98.
5. Grandhi MS, Kim AK, Ronnekleiv-Kelly SM, Kamel IR, Ghasebeh MA, Pawlik TM. Hepatocellular carcinoma: From diagnosis to treatment. Surg Oncol. 2016;25:74–85.
6. Liu P, Hsu C, Hsia C, Lee Y, Su C, Huang Y, Lee F, Lin H, Huo T. Prognosis of hepatocellular carcinoma: Assessment of eleven staging systems. Journal of hepatology. 2016;64:601–8.
7. Chen L, Chang Y, Chang Y Survival Predictability Between the American Joint Committee on Cancer 8th Edition Staging System and the Barcelona Clinic Liver Cancer Classification in Patients with Hepatocellular Carcinoma. The oncologist 2020.
8. Zhang Q, Lou Y, Yang J, Wang J, Feng J, Zhao Y, Wang L, Huang X, Fu Q, Ye M, Zhang X, Chen Y, Ma C, Ge H, Wang J, Wu J, Wei T, Chen Q, Wu J, Yu C, Xiao Y, Feng X, Guo G, Liang T, Bai X. Integrated multiomic analysis reveals comprehensive tumour heterogeneity and novel immunophenotypic classification in hepatocellular carcinomas. Gut. 2019;68:2019–31.
9. Ringelhan M, Pfister D, O'Connor T, Pikarsky E, Heikenwalder M. The immunology of hepatocellular carcinoma. Nat Immunol. 2018;19:222–32.
10. Grosser R, Cherkassky L, Chintala N, Adusumilli PS. Combination Immunotherapy with CAR T Cells and Checkpoint Blockade for the Treatment of Solid Tumors. Cancer Cell. 2019;36:471–82.
11. Cheng H, Sun G, Chen H, Li Y, Han Z, Li Y, Zhang P, Yang L, Li Y. Trends in the treatment of advanced hepatocellular carcinoma: immune checkpoint blockade immunotherapy and related combination

therapies. American journal of cancer research. 2019;9:1536–45.
12. Nilsen T, Graveley B. Expansion of the eukaryotic proteome by alternative splicing. Nature. 2010;463:457–63.
13. Black D. Mechanisms of alternative pre-messenger RNA splicing. Annual review of biochemistry. 2003;72:291–336.
14. Li Y, Sun N, Lu Z, Sun S, Huang J, Chen Z, He J. Prognostic alternative mRNA splicing signature in non-small cell lung cancer. Cancer letters. 2017;393:40–51.
15. Calabrese C, Davidson N, Demircioğlu D, Fonseca N, He Y, Kahles A, Lehmann K, Liu F, Shiraishi Y, Soulette C, Urban L, Greger L, Li S, Liu D, Perry M, Xiang Q, Zhang F, Zhang J, Bailey P, Erkek S, Hoadley K, Hou Y, Huska M, Kilpinen H, Korbel J, Marin M, Markowski J, Nandi T, Pan-Hammarström Q, Pedamallu C, Siebert R, Stark S, Su H, Tan P, Waszak S, Yung C, Zhu S, Awadalla P, Creighton C, Meyerson M, Ouellette B, Wu K, Yang H, Brazma A, Brooks A, Göke J, Rätsch G, Schwarz R. Stegle O and Zhang Z. Genomic basis for RNA alterations in cancer. Nature. 2020;578:129–36.
16. Climente-González H, Porta-Pardo E, Godzik A, Eyras E. The Functional Impact of Alternative Splicing in Cancer. Cell reports. 2017;20:2215–26.
17. Lee SC, Abdel-Wahab O. Therapeutic targeting of splicing in cancer. Nat Med. 2016;22:976–86.
18. Tripathi V, Ellis J, Shen Z, Song D, Pan Q, Watt A, Freier S, Bennett C, Sharma A, Bubulya P, Blencowe B, Prasanth S, Prasanth K. The nuclear-retained noncoding RNA MALAT1 regulates alternative splicing by modulating SR splicing factor phosphorylation. Molecular cell. 2010;39:925–38.
19. El Marabti E, Younis I. The Cancer Spliceome: Reprograming of Alternative Splicing in Cancer. Frontiers in molecular biosciences. 2018;5:80.
20. Yang Q, Zhao J, Zhang W, Chen D, Wang Y. Aberrant alternative splicing in breast cancer. J Mol Cell Biol. 2019;11:920–9.
21. Li S, Hu Z, Zhao Y, Huang S, He X. Transcriptome-Wide Analysis Reveals the Landscape of Aberrant Alternative Splicing Events in Liver Cancer. Hepatology. 2019;69:359–75.
22. Lee SE, Alcedo KP, Kim HJ, Snider NT. Alternative Splicing in Hepatocellular Carcinoma. Cell Mol Gastroenterol Hepatol. 2020;10:699–712.
23. Zhu G, Zhou Y, Qiu L, Wang B, Yang Y, Liao W, Luo Y, Shi Y, Zhou J, Fan J, Dai Z. Prognostic alternative mRNA splicing signature in hepatocellular carcinoma: a study based on large-scale sequencing data. Carcinogenesis 2019.
24. Cai Y, Xia J, Wang N, Zhou H. Identification of prognostic alternative splicing signatures in hepatitis B or/and C viruses related hepatocellular carcinoma. Genomics. 2020;112:3396–406.
25. Blanche P, Dartigues J, Jacqmin-Gadda H. Estimating and comparing time-dependent areas under receiver operating characteristic curves for censored event times with competing risks. Statistics in medicine. 2013;32:5381–97.
26. Goodman A, Patel S, Kurzrock R. PD-1-PD-L1 immune-checkpoint blockade in B-cell lymphomas. Nat Rev Clin Oncol. 2017;14:203–20.

27. Kim J, Patel M, Mangraviti A, Kim E, Theodros D, Velarde E, Liu A, Sankey E, Tam A, Xu H, Mathios D, Jackson C, Harris-Bookman S, Garzon-Muvdi T, Sheu M, Martin A, Tyler B, Tran P, Ye X, Olivi A, Taube J, Burger P, Drake C, Brem H. Pardoll D and Lim M. Combination Therapy with Anti-PD-1, Anti-TIM-3, and Focal Radiation Results in Regression of Murine Gliomas. Clinical cancer research: an official journal of the American Association for Cancer Research. 2017;23:124–36.
28. Nishino M, Ramaiya N, Hatabu H, Hodi F. Monitoring immune-checkpoint blockade: response evaluation and biomarker development. Nat Rev Clin Oncol. 2017;14:655–68.
29. Zhai L, Ladomersky E, Lenzen A, Nguyen B, Patel R, Lauing K, Wu M, Wainwright. D. IDO1 in cancer: a Gemini of immune checkpoints. Cell Mol Immunol. 2018;15:447–57.
30. Seiler M, Peng S, Agrawal A, Palacino J, Teng T, Zhu P, Smith P, Buonamici S, Yu L. Somatic Mutational Landscape of Splicing Factor Genes and Their Functional Consequences across 33 Cancer Types. Cell reports. 2018;23:282–96.e284.
31. Llovet J, Montal R, Sia D, Finn R. Molecular therapies and precision medicine for hepatocellular carcinoma. Nat Rev Clin Oncol. 2018;15:599–616.
32. Pitt J, Vétizou M, Daillère R, Roberti M, Yamazaki T, Routy B, Lepage P, Boneca I, Chamaillard M, Kroemer G, Zitvogel L. Resistance Mechanisms to Immune-Checkpoint Blockade in Cancer: Tumor-Intrinsic and -Extrinsic Factors. Immunity. 2016;44:1255–69.
33. Salik B, Smyth M, Nakamura K. Targeting immune checkpoints in hematological malignancies. J Hematol Oncol. 2020;13:111.
34. Comprehensive and Integrative Genomic Characterization of Hepatocellular. Carcinoma Cell. 2017;169:1327–41.e1323.
35. Schulze K, Nault J, Villanueva A. Genetic profiling of hepatocellular carcinoma using next-generation sequencing. Journal of hepatology. 2016;65:1031–42.
36. Woo H, Kim Y. Multiplatform Genomic Roadmap of Hepatocellular Carcinoma: A Matter of Molecular Heterogeneity. Hepatology. 2018;68:2029–32.
37. Prieto J, Melero I, Sangro B. Immunological landscape and immunotherapy of hepatocellular carcinoma. Nat Rev Gastroenterol Hepatol. 2015;12:681–700.
38. Lu Y, Xu W, Ji J, Feng D, Sourbier C, Yang Y, Qu J, Zeng Z, Wang C, Chang X, Chen Y, Mishra A, Xu M, Lee M, Lee S, Trepel J, Linehan W, Wang X, Yang Y, Neckers L. Alternative splicing of the cell fate determinant Numb in hepatocellular carcinoma. Hepatology. 2015;62:1122–31.
39. Abrami L, Dallavilla T, Sandoz P, Demir M, Kunz B, Savoglidis G, Hatzimanikatis V, van der Goot F. Identification and dynamics of the human ZDHHC16-ZDHHC6 palmitoylation cascade. eLife 2017; 6.
40. Shi W, Chen X, Wang F, Gao M, Yang Y, Du Z, Wang C, Yao Y, He K, Hao A. ZDHHC16 modulates FGF/ERK dependent proliferation of neural stem/progenitor cells in the zebrafish telencephalon. Developmental neurobiology. 2016;76:1014–28.
41. Cao N, Li J, Rao Y, Liu H, Wu J, Li B, Zhao P, Zeng L, Li J. A potential role for protein palmitoylation and zDHHC16 in DNA damage response. BMC Mol Biol. 2016;17:12.

Tables

TABLE 1 | Baseline data of all HCC patients.

Characteristic	Type	n	Proportion(%)
Age	<=65	235	62.33%
	>65	141	37.40%
	unknow	1	0.27%
Gender	FEMALE	122	32.36%
	MALE	255	67.64%
Grade	G1-2	235	62.33%
	G3-4	137	36.34%
	unknow	5	1.33%
Stage	Stage I-II	262	69.50%
	Stage III-IV	91	24.14%
	unknow	24	6.37%
T stage	T1-2	280	74.27%
	T3-4	94	24.93%
	unknow	3	0.80%
M stage	M0	272	72.15%
	M1	4	1.06%
	unknow	101	26.79%
N stage	N0	257	68.17%
	N1	4	1.06%
	unknow	116	30.77%

Figures

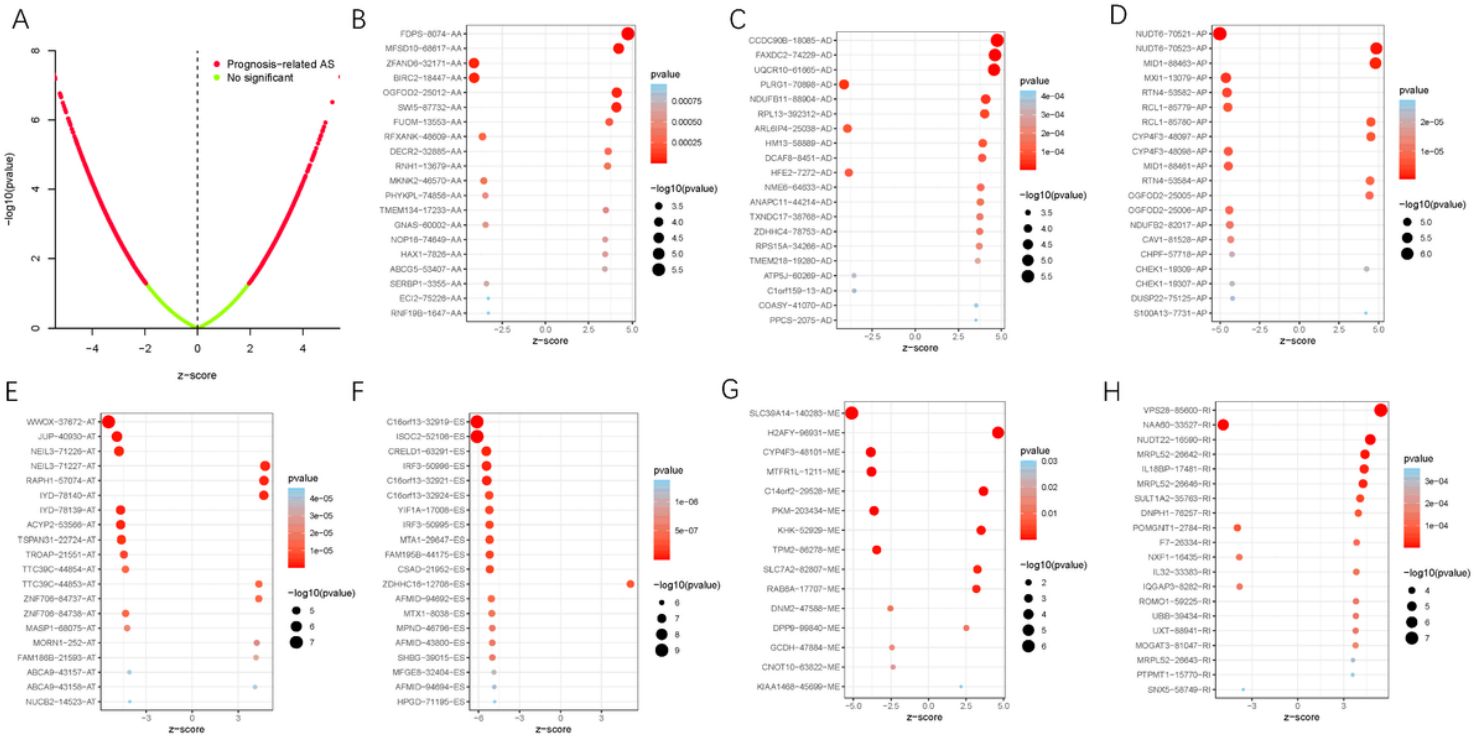

Figure 1

The survival-relevant AS events. (A) The volcano plots of survival-relevant AS events. The most significant survival-relevant AAs, ADs, APs, ATs, ESs, MEs and RIs in TCGA LIHC cohort (B-H).

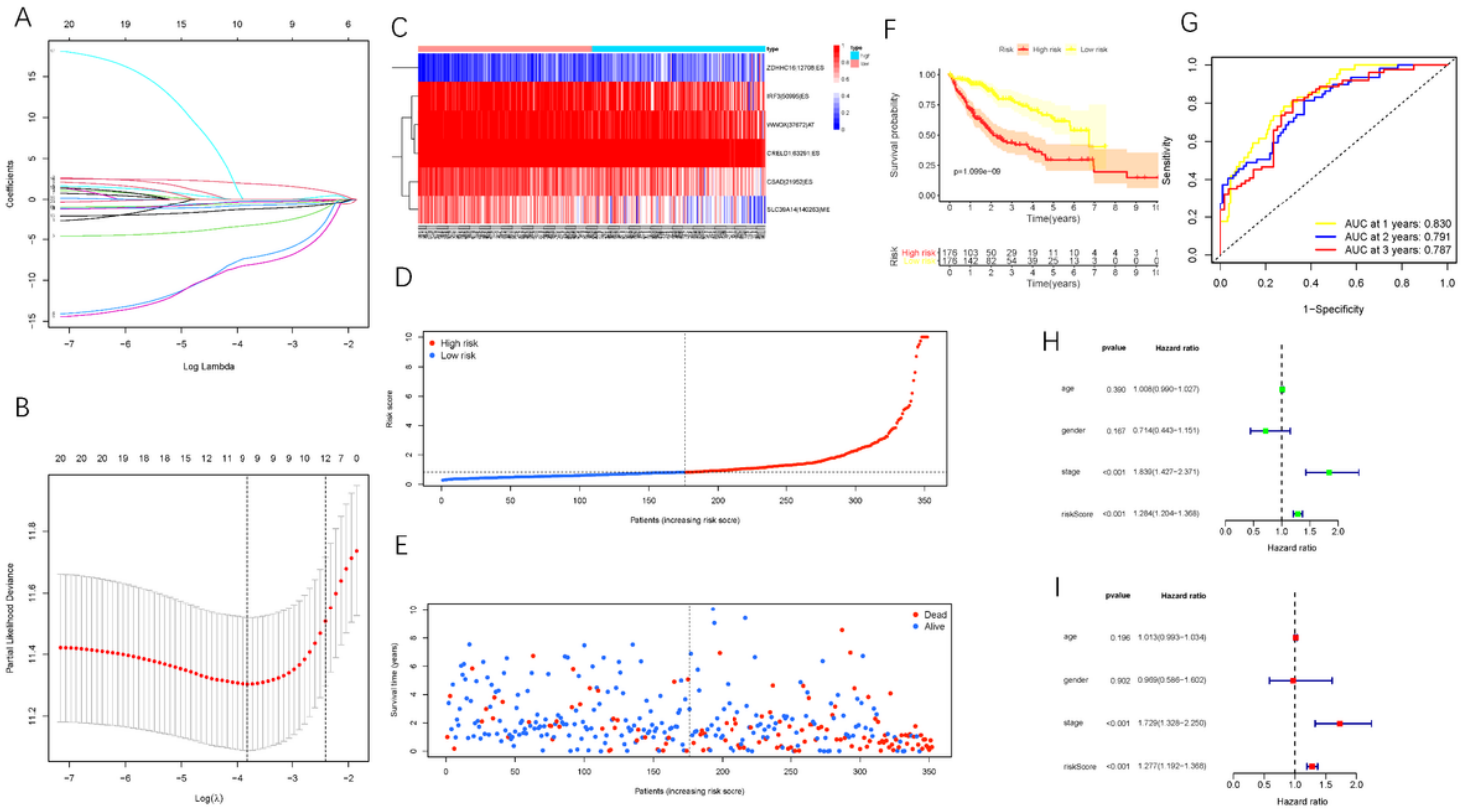

Figure 2

Confirmation of ALL AS-based prognostic signature. (A) LASSO coefficient profiles of the whole AS events. (B) Ten-time cross-validation for tuning parameter selection in the lasso regression. (C) Heatmap of the ALL signature AS events PSI value in HCC. The color from red to blue shows a trend from high expression to low expression. (D) Distribution of ALL signature risk score. (E) The survival status and duration of HCC patients. (F) Kaplan–Meier curve presenting survival in the high-risk and low-risk sets. (G) ROC analysis of the risk scores for overall survival prediction. The AUC was calculated for ROC curves, and sensitivity and specificity were calculated to assess score performance. Proportional hazards model results. (H) Univariate Cox regression results. (I) Multivariate Cox regression results.

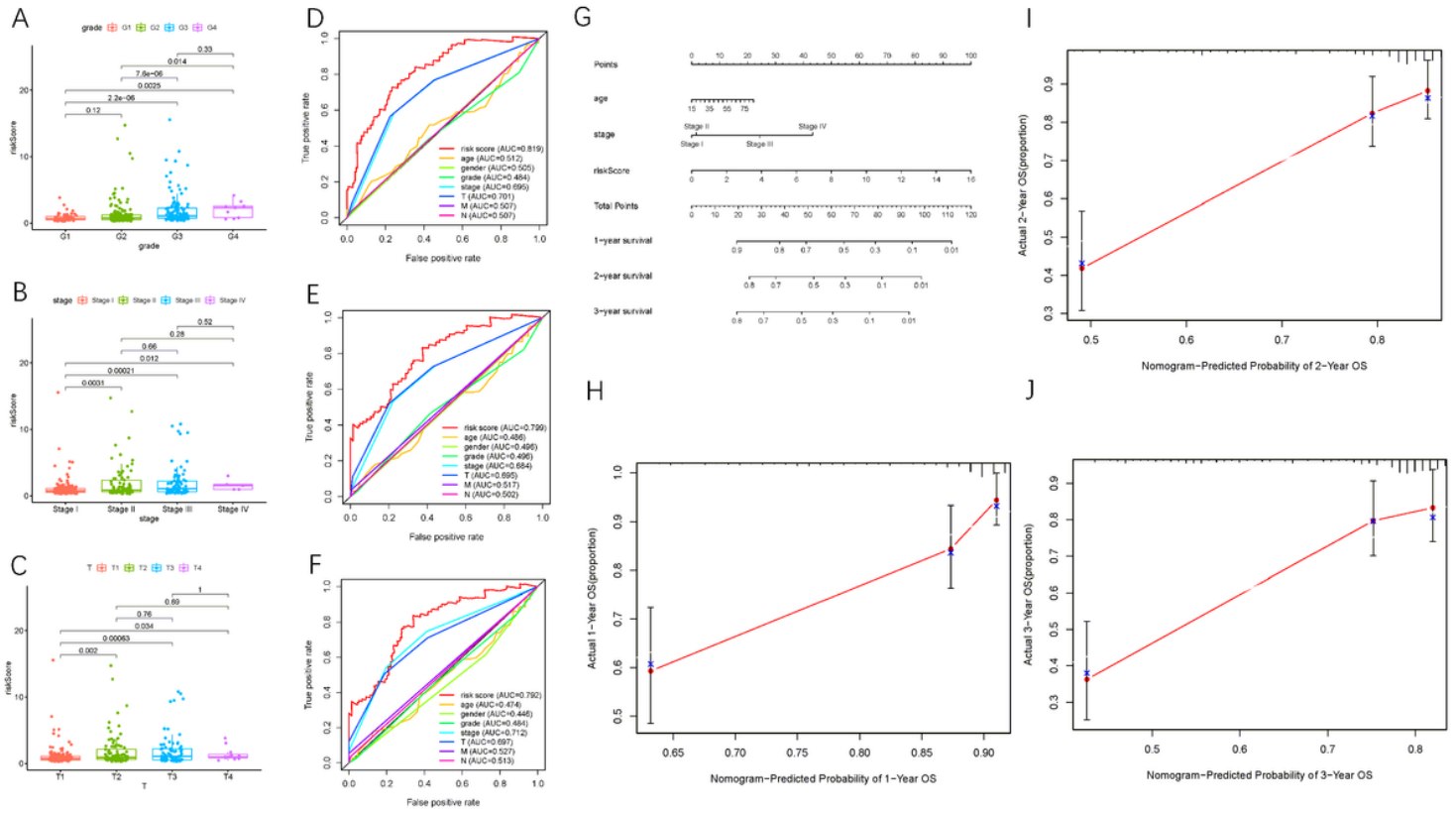

Figure 3

Validation of prognostic value of ALL AS-based prognostic signature. (A) Correlation of risk score with tumor grade. (B) Correlation of risk score with clinicopathological. (C) Correlation of risk score with T status. (D-F) Areas under curves (AUCs) for predicting 1-, 2-, and 3-year survival with different clinical characteristics. (G) Nomogram was assembled by stage and risk signature for predicting survival of HCC patients. (H) One-year nomogram calibration curves. (I) Two-year nomogram calibration curves. (J) Three-year nomogram calibration curves.

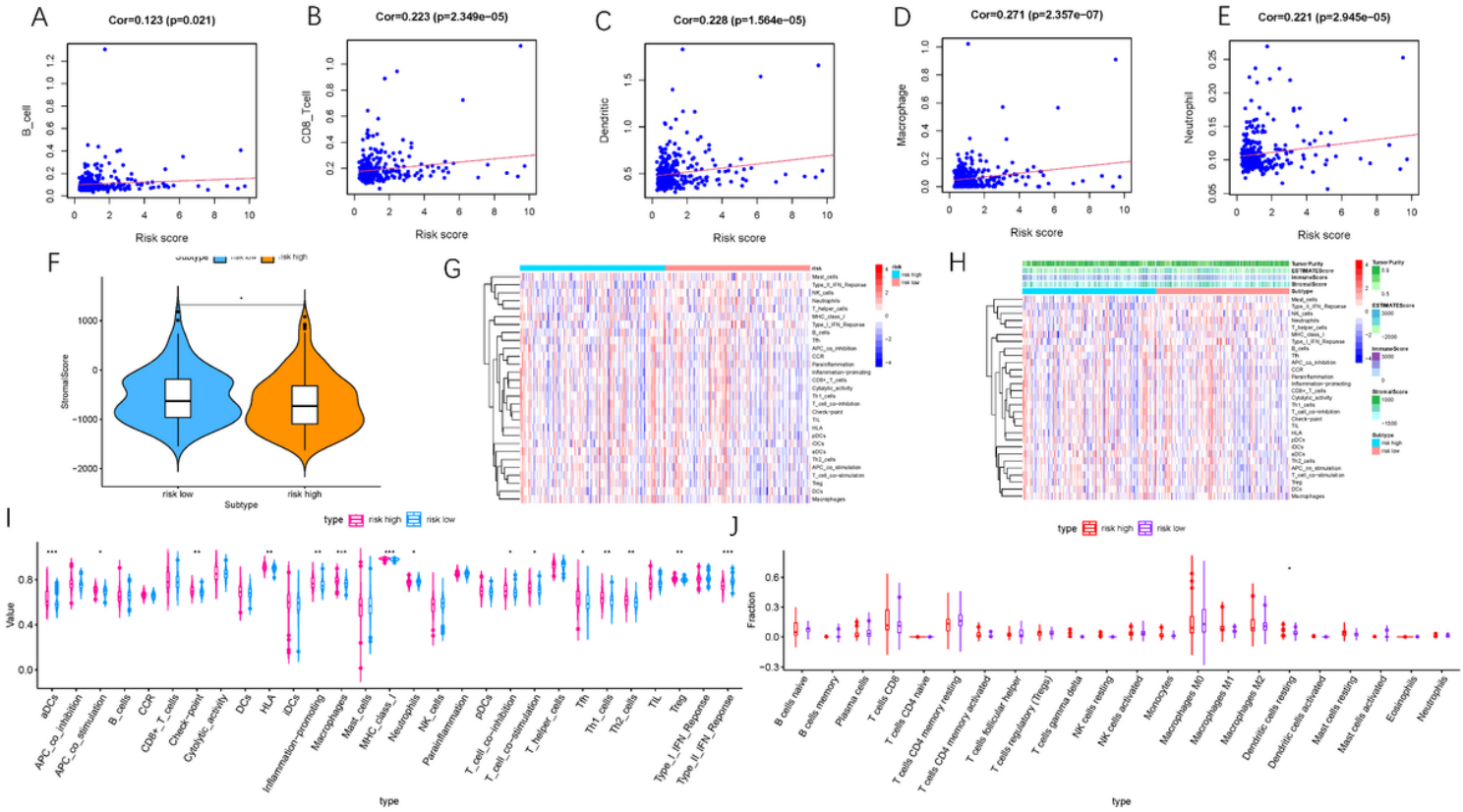

Figure 4

Correlation between infiltrating immune cells and ALL AS-based prognostic signature. (A)Relationship between this signature and B cells. (B) Relationship between this signature and CD8+T cells. (C) Relationship between this signature and Dendritic cells. (D) Relationship between this signature and Macrophages. (E) Relationship between this signature and Neutrophils. (F) Comparison of stromal score between low- and high-risk groups. (G)Heatmap displayed enrichment of 29 immune signatures of low-/high-risk groups. Blue represents low activity and red represent high activity. (H)Heatmap of 29 immune signatures and immune scores of two different risk score groups. Blue represents low activity and red represent high activity. (I) Distinction of enrichment of immune-related signatures between risk-low and risk-high groups. (J) Difference of infiltrating immune cell subpopulations and levels between low-/high-risk groups.

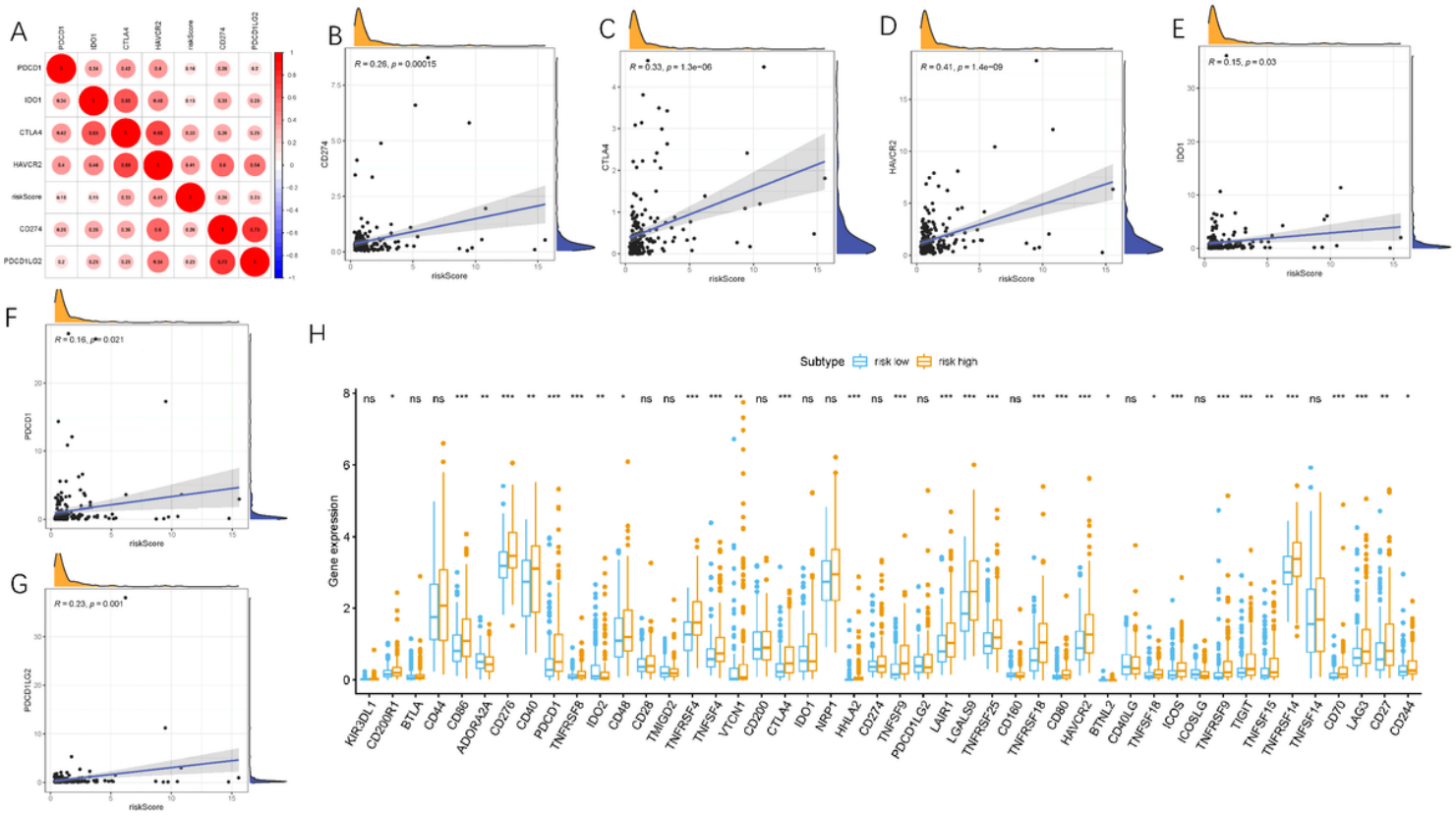

Figure 5

Association between ALL AS-based prognostic signature and crucial immune checkpoint genes. (A) association analyses between immune checkpoint inhibitors CD274, PDCD1, PDCD1LG2, CTLA4, HAVCR2, and IDO1 and risk score. (B) association between risk score and CD274. (C) association between risk score and CTLA4. (D) association between risk score and HAVCR2. (E) association between risk score and IDO1. (F) association between risk score and PDCD1. (G) association between risk score and PDCD1LG2. (H) Comparison of immune checkpoint blockade-related genes expression levels between low-risk group and high-risk groups.

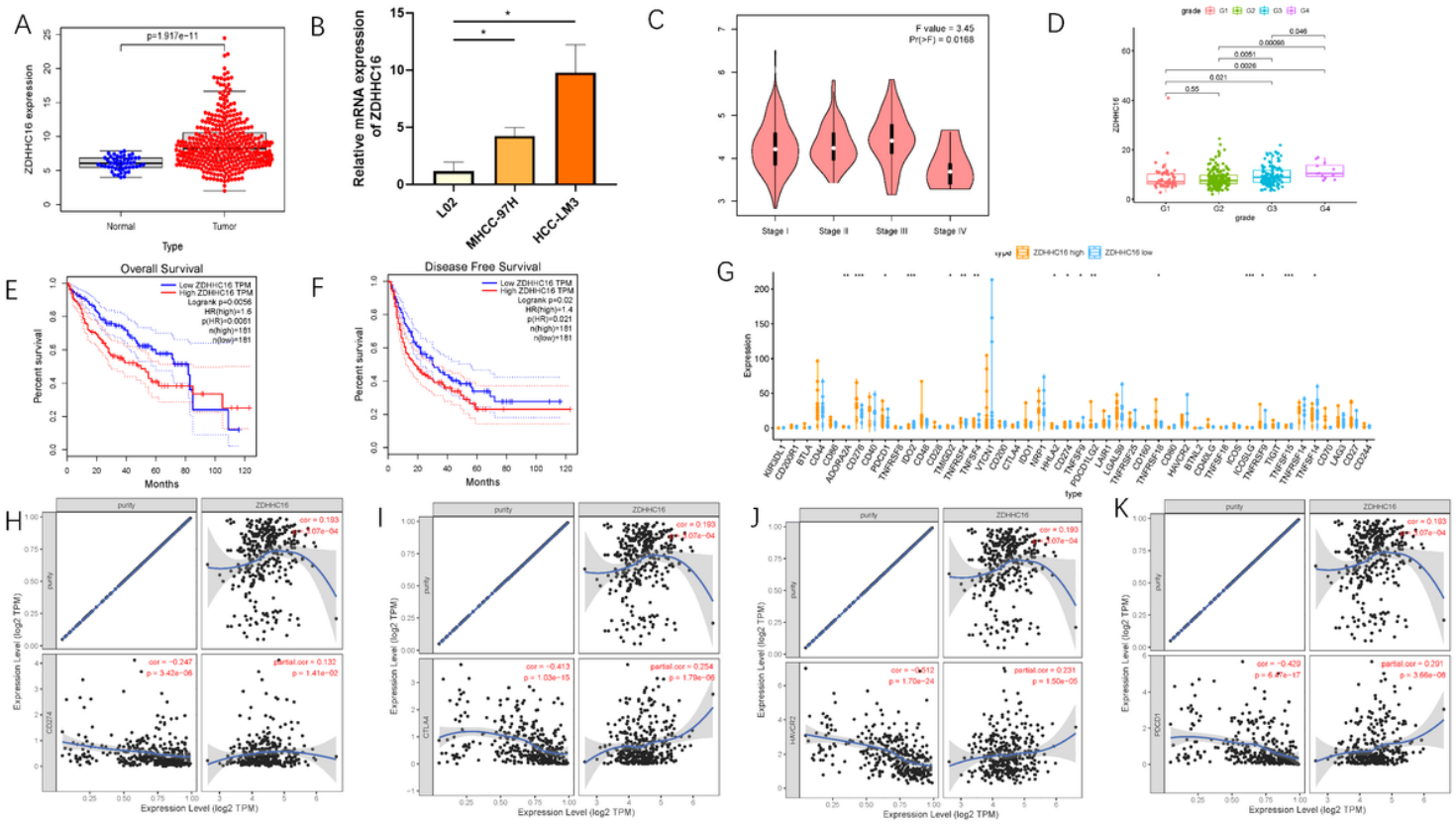

Figure 6

The clinical significance of ZDHHC16 in HCC and in vitro study. ZDHHC16 are overexpressed in HCC tumor tissue (A) and HCC cell lines (B). (C) The expression of ZDHHC16 had significant difference between major pathological stages. (D) Correlation of risk score with tumor grade. Lower ZDHHC16 level predicts longer overall survival (E) and disease-free survival (F). (G) Comparison of immune checkpoint blockade-related genes expression levels between low-ZDHHC16 group and high-ZDHHC16 group. (H) Correlation of risk score with CD274. (I) Correlation of risk score with CTLA4. (J) Correlation of risk score with HAVCR2. (K) Correlation of risk score with PDCD1.

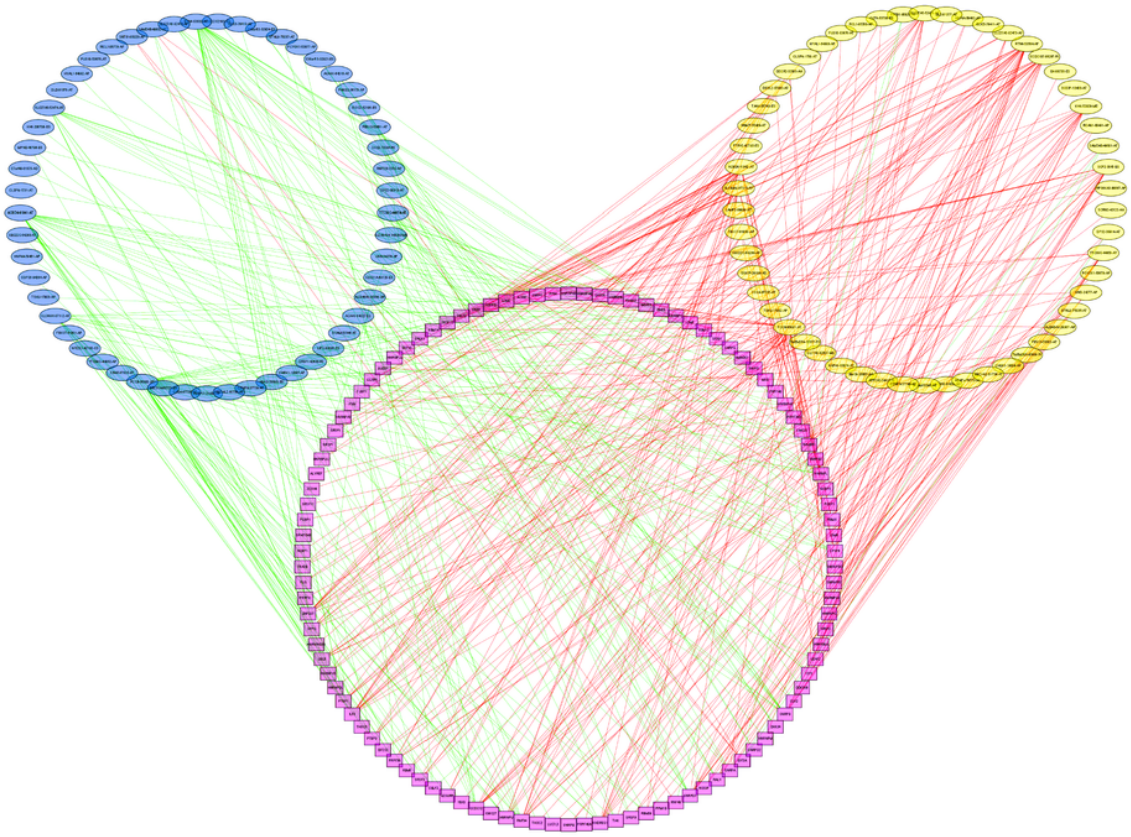

Figure 7

The regulatory network between SFs and survival related AS events. The yellow or blue ellipses indicated the AS events positively or negatively correlated with survival. Purple rectangles represented SFs. The positive/negative correlations (r>0.6 or r<-0.6) between SFs and AS events were indicated with red/green lines.

Supplementary Files

This is a list of supplementary files associated with this preprint. Click to download.

- supplementarymaterials.rar